NdFeAs(O,H) epitaxial thin films with high critical current density

Keisuke Kondo[1], Seiya Motoki[1], Takafumi Hatano[1], Takahiro Urata[1], Kazumasa Iida[1,2], Hiroshi Ikuta[1]

Department of Materials Physics, Nagoya University, Japan[1]

JST CREST, Japan[2]

Abstract

We report on the growth of NdFeAs(O,H) epitaxial thin films on MgO (001) substrates and their electrical transport properties. The maximum carrier density of the NdFeAs(O,H) films was more than twice larger than that of our NdFeAs(O,F) films. This enabled us to investigate the physical properties of heavily electron doped NdFeAsO, which could not be achieved with NdFeAs(O,F). The irreversibility field H_{irr} of NdFeAs(O,H) was larger than that of NdFeAs(O,F) for $H \parallel c$ due to the decrease in the anisotropy of the upper critical field. A very high critical current density of 17 MA/cm^2 was recorded at 4 K, which corresponds to about 13% of the depairing current density of NdFeAs(O,F).

1. Introduction

Fe-based superconductors exhibit the highest superconducting transition temperature (T_c) at ambient pressure apart from cuprates, and have been energetically investigated from basic science and engineering points of view. Among them, *Ln*FeAsO (*Ln* : lanthanoid elements) is an attractive material class because it exhibits the highest T_c up to 58 K by substituting F or H for O [1-3]. For the *Ae*Fe_2As_2 (*Ae* : alkali earth elements) systems, the electronic phase diagrams have been reported for various doping elements, and the physical properties have been investigated in a wide range of doping levels [4]. For *Ln*$FeAsO_{1-x}F_x$, however, the solubility limit of F is around x=0.2 [2], and it is not possible to explore the superconducting properties of heavily F doped *Ln*FeAsO. On the other hand, it was reported that the substitution limit can be increased up to x~0.8 by doping H instead of F, while the maximum T_c of *Ln*FeAs(O,H) was comparable to that of *Ln*FeAs(O,F) [3,5]. However, the available size of single crystals is still small, which makes detailed measurements of the fundamental physical properties not easy. For instance, it was necessary to machine a tiny bar by focused ion beam to investigate the anisotropy of the electronic transport properties because the typical size of the single crystal was ~200×200×10 μm^3 [6].

Recently, a novel method of doping H into SmFeAsO epitaxial thin films using a topotactic reaction was reported [7]. This opens new opportunities to investigate the physical properties of heavily electron doped *Ln*FeAsO. Previously, we established a method for growing high quality NdFeAsO

epitaxial thin films by molecular beam epitaxy (MBE) [8,9]. In the present study, we doped H to the MBE-grown NdFeAsO thin films for investigating the physical properties in the overdoped region. We found that the overdoped NdFeAs(O,H) thin films have a larger irreversibility field H_{irr} and critical current density J_c than NdFeAs(O,F) thin films.

2. Experimental procedure

Parent NdFeAsO thin films were fabricated on MgO (001) at 800°C by MBE. Solid sources of Fe, As, NdF_3, Fe_2O_3 and Ga were charged in Knudsen cells. Here, Fe_2O_3 was the oxygen source and Ga was used as a F-getter via the following reaction: $Ga + NdF_3 \rightarrow Nd + GaF_3$ [10]. The thickness of all NdFeAsO thin films was measured by small-angle X-ray scattering, and was confirmed to be 20-30 nm. H-doping into the NdFeAsO thin films was conducted by referring to Ref. 7. The NdFeAsO thin films were cut into small specimens of about 5×5 mm^2 and sealed in an evacuated quartz tube filled with CaH_2 powder as a hydrogen source. The whole arrangement was then heated under various conditions in order to optimize the H-doping process. For comparative studies, F-doped NdFeAsO thin films were fabricated by a two-step method, i.e. a NdOF layer was deposited on the parent NdFeAsO phase for F doping as reported in Ref. 10. Phase purity and crystalline quality of the fabricated thin films were examined by X-ray diffraction using Cu Kα radiation. The temperature dependence of the resistance was measured by a four-probe method, and the carrier density at 50 K was determined by Hall measurements in the field range up to $\mu_0 H = \pm 9$ T.

The films were photolithographically patterned by Ar-ion milling to form 20 μm-wide and 1 mm-long bridges for resistivity and current-voltage characteristics measurements. From the temperature and magnetic field dependence of resistivity $\rho(H, T)$, the upper critical field H_{c2} and T_c^{onset} was deduced. The irreversibility field H_{irr} was determined with a criterion of $\rho=10^{-5}$ mΩcm. The critical current density J_c was determined using an electric field criterion of E=1 μV/cm from the current-voltage characteristics.

3. Results and discussion

In order to optimize the H-doping process, the processing temperature (T_{proc}) was varied as 390°C, 440°C, and 490°C, while the duration time was fixed at 8 hours. Figure 1(a) shows the $\theta/2\theta$ scans of the resultant films. The dashed lines in Fig. 1(a) indicate the positions of the 00l peaks of the non-doped NdFeAsO thin film. No impurities were detected irrespective of the processing temperature. The positions of the 00l peaks for the films processed at 390°C and 440°C did not change, whereas the corresponding positions of the film processed at 490°C shifted to higher angles. The c-axis length determined from the positions of the 00l peaks using the Nelson-Riley function [11] did not change for the films processed at 390°C and 440°C compared to the non-doped NdFeAsO thin film. However, the c-axis length of the film processed at 490°C decreased from 8.575Å to 8.545 Å. The study of bulk

SmFeAs(O,H) showed that the *c*-axis length decreases with H doping [4]. Hence, the above result can be taken as an evidence that H was doped into the NdFeAsO thin film. Furthermore, the temperature dependence of resistance (Fig. 1(b)) shows that only the sample processed at 490°C exhibited a superconducting transition at $T_c^{onset} = 46$ K and $T_c^0 = 43$ K. When T_{proc} was further increased to 520°C, the quartz tube ruptured due to the increase of internal pressure. Therefore, the optimal processing temperature was 490°C within our experimental condition.

Next, the processing time (t_{proc}) was changed from 8 to 72 hours at 490°C. Figure 2 shows the *c*-axis length of the resultant film as a function of t_{proc}. As can be seen, the *c*-axis length decreased monotonously with t_{proc} until ~20 h. For $t_{proc} \geq 20$ h, the *c*-axis length was almost constant. Therefore, it can be concluded that the duration at 490°C requires more than 20 hours to sufficiently dope hydrogen into the NdFeAsO thin films.

Figure 3(a) shows the *c*-axis length dependence of T_c^{onset} for the NdFeAs(O,H) thin films obtained from the resistance measurements. For comparison, the data of our NdFeAs(O,F) thin films are also shown. The T_c^{onset} of the NdFeAs(O,H) thin films was almost constant at around 47 K in the range of 8.43 Å $\leq c \leq$ 8.54 Å. Because the *c*-axis lattice parameter correlates with the carrier density, this result resembles the T_c plateau in the phase diagram of SmFeAs(O,H) and CeFeAs(O,H) [3,12]. In addition, NdFeAs(O,H) films having a *c*-axis length much smaller than NdFeAs(O,F) films were obtained. Figure 3(b) shows the carrier density *n* determined from the Hall effect measurements at 50 K as a function of the *c*-axis length for the same thin films. The Hall coefficients for all samples were negative, indicating that the dominant carrier was electron. The carrier density of NdFeAs(O,H) at 50 K increased as the *c*-axis length became smaller. Compared with a NdFeAs(O,F) film having a similar T_c of ~ 47 K, the carrier density of the NdFeAs(O,H) film was more than twice larger. These results indicate that a higher carrier density can be achieved with H-doping.

The data regarding the crystalline quality of the NdFeAs(O,H) film prepared under the optimized condition determined above (T_{proc} = 490°C and t_{proc} = 36 h) are shown in Fig. 4. Note that the NdFeAs(O,H) film was confirmed to be *c*-axis oriented and impurity free by $\theta/2\theta$ scan (not shown). As can be seen, sharp peaks were observed at every 90° in the ϕ scan of the 200 reflection, resulting from the tetragonal symmetry of NdFeAs(O,H). These results prove that the film was epitaxially grown on the MgO substrate. The average of the full width at half maximum value $\Delta\phi$ of the peaks was $\Delta\phi = 0.84°$. Further, the ω-scan of the 003 peak showed a sharp full width at half maximum value $\Delta\omega$ of 0.77°. Both $\Delta\phi$ and $\Delta\omega$ of the NdFeAs(O,H) film are almost equivalent to those of the non-doped NdFeAsO thin film, indicative of good crystallinity.

Figure 5(a) exhibits the ρ-T curve of the NdFeAs(O,H) thin film shown in Fig. 4. The ρ-T curve showed a sharp superconducting transition at $T_c^{onset} = 46$ K and $T_c^0 = 43$ K. In addition, the ratio of the resistivity at 300 K to that at 50 K was 8.7, which is higher than that of our NdFeAs(O,F) films, suggesting that the film is of good quality. In order to draw the magnetic phase diagram, ρ-T curves

were measured in various magnetic fields up to 9 T applied parallel to the crystallographic *c*-axis ($H \parallel c$) and *ab*-plane ($H \parallel ab$) (Figs. 5(b) and (c)). The resultant phase diagrams are summarized in Figs. 5(d) and (e). Here the temperature was normalized by T_c^{onset} for the upper critical field (H_{c2}) and T_{irr} for the irreversibility field (H_{irr}) at 0 T [i.e. $\rho(0, T_{irr}) = 10^{-5}$ mΩcm], respectively. For comparison, the data of our NdFeAs(O,F) film ($T_c^{onset} = 45$ K and $T_c^0 = 40$ K) are also plotted [13]. The H_{c2} for $H \parallel ab$ of NdFeAs(O,H) was comparable to that of NdFeAs(O,F), but for $H \parallel c$ NdFeAs(O,H) showed a higher H_{c2} than NdFeAs(O,F). The respective H_{c2} anisotropies for NdFeAs(O,H) and NdFeAs(O,F) are 4.5 and 5.1, which were evaluated by the slope of $H_{c2}(T)$. On the other hand, the irreversibility fields of NdFeAs(O,H) are higher than those of NdFeAs(O,F) for both main crystallographic orientations. For cuprate superconductors, it has been shown that the irreversibility field for $H \parallel c$ increases with doping when compared at the same normalized temperature because of the decrease in the electromagnetic anisotropy [14]. The enhanced H_{irr} for NdFeAs(O,H) may be explained similarly. For $H \parallel ab$, the reason for the improvement of H_{irr} is not clear. Further investigation is necessary to clarify this point.

The field dependence of the critical current density J_c for NdFeAs(O,H) measured at various temperatures is shown in Fig. 5(d). Self-field J_cs of 17 MA/cm^2 and 2.9 MA/cm^2 were recorded at 4 K and 32 K, respectively. These values are higher than those of our ordinary NdFeAs(O,F) films [15]. The depairing current density J_d of NdFeAs(O,H) cannot be estimated due to the lack of the penetration depth measurement, but the value of J_c at 4 K corresponds to 13% of J_d of NdFeAs(O,F). Here J_d was estimated using the following formula [16]: $\phi_0/3\sqrt{3}\pi\mu_0\lambda_{ab}^2\xi_{ab} \sim 137$ MA/cm^2 at 0 K, where ϕ_0 is the magnetic flux quantization, μ_0 is the permeability in vacuum, λ_{ab} is the in-plane penetration length (195 nm [17]), and ξ_{ab} is the coherence length (1.93 nm [15]) of the NdFeAs(O,F) thin film. The highest J_c reported to date for iron-based superconductors is 20 MA/cm^2 (at $T = 5$ K) of SmFeAs (O, F) with columnar defects introduced by ion irradiation [18]. In our NdFeAs(O,H) thin film, J_c was close to that value even though no defect was intentionally introduced. J_c decreased monotonously as the magnetic field was increased, but maintained a high value of 1.6 MA/cm^2 at 4 K even at a high magnetic field of 9 T. From these results, overdoped *Ln*FeAs(O,H) can be expected to show high potential for wire applications in high magnetic field.

4. Conclusion

In summary, NdFeAs(O,H) epitaxial thin films were successfully fabricated and their electrical transport properties were investigated. The maximum carrier density of the NdFeAs(O,H) films was more than twice larger than that of NdFeAs(O,F). The H_{irr} of NdFeAs(O,H) was larger than that of NdFeAs(O,F) due to the decrease in the anisotropy of the upper critical field. A self-field J_c of 17 MA/cm^2 was recorded at 4 K, which is 13% of the depairing current density of NdFeAs(O,F).

Acknowledgment

This work was supported by JST CREST Grant Number JPMJCR18J4.

The data that support the findings of this study are available from the corresponding author upon reasonable request.

References

[1] Y. Kamihara, T. Watanabe, M. Hirano, and H. Hosono, *J. Am Chem. Soc.* **130**, 3296 (2008).

[2] M. Fujioka, S. J. Denholme, T. Ozaki, H. Okazaki, K. Deguchi, S. Demura, H. Hara, T. Watanabe, H. Takeya, T. Yamaguchi, H. Kumakura and Y. Takano, *Supercond. Sci. Technol.* **26**, 085023 (2013).

[3] T. Hanna, Y. Muraba, S. Matsuishi, N. Igawa, K. Kodama, S. Shamoto, and H. Hosono, *Phys. Rev. B* **84**, 024521 (2011).

[4] S. Ishida, D. Song, H. Ogino, A. Iyo, H. Eisaki, M. Nakajima, J. Shimoyama, and M.Eisterer *Phys. Rev. B* **95**, 014517 (2017).

[5] S. Iimura, H. Okanishi, S. Matsuishi, H. Hiraka, T. Honda, K. Ikeda, T. C. Hansen, T. Otomo, and H. Hosono, *Proc. Natl. Acad. Sci. USA* **114**, E4354 (2017).

[6] S. Iimura, T. Muramoto, S. Fujitsu, S. Matsuishi, and H. Hosono, *J. Asian Ceram. Soc.* **5**, 357 (2017).

[7] J. Matsumoto, K. Hanzawa, M. Sasase, S. Haindl, T. Katase, H. Hiramatsu, and H. Hosono, *Phys. Rev. Materials* **3**, 103401 (2019).

[8] T. Kawaguchi, H. Uemura, T. Ohno, R. Watanabe, M. Tabuchi, T. Ujihara, K. Takenaka, Y. Takeda, and H. Ikuta, *Appl. Phys. Express* **2** 093002 (2009).

[9] T. Kawaguchi, H. Uemura, T. Ohno, M. Tabuchi, T. Ujihara, K. Takenaka, Y. Takeda, and H. Ikuta, *Appl. Phys. Lett*. **97**, 042509 (2010).

[10] T. Kawaguchi, H. Uemura, T. Ohno, M. Tabuchi, T. Ujihara, Y. Takeda and H. Ikuta, *Appl. Phys. Express* **4** 083102 (2011).

[11] J. B. Nelson and D. P. Riley, *Proc. Phys. Soc.* **57**, 160 (1945).

[12] S. Matsuishi, T. Hanna, Y. Muraba, S. W. Kim, J. E. Kim, M. Takata, S. Shamoto, R. I. Smith, and H. Hosono, *Phys. Rev. B* **85**, 014514 (2012).

[13] S. Kauffmann-Weiss, K. Iida, C. Tarantini, T. Boll, R. Schneider, T. Ohmura, T. Matsumoto, T. Hatano, M. Langer, S. Meyer, J. Jaroszynski, D. Gerthsen, H. Ikuta, B. Holzapfel and J. Hänisch, *Nanoscale Adv.*, **1**, 3036 (2019).

[14] K. Kitazawa, J. Shimoyama, H. Ikuta, T. Sasagawa and K. Kishio, *Physica C* **282-287**, 335 (1997).

[15] C. Tarantini, K. Iida, J. Hänisch, F. Kurth, J. Jaroszynski, N. Sumiya, M. Chihara, T. Hatano, H. Ikuta, S. Schmidt, P. Seidel, B. Holzapfel and D. C. Larbalestier, *Sci. Rep.* **6**, 36047 (2016).

[16] G. Blatter, M. V. Feigel'man, V. B. Geshkenbein, A. I. Larkin and V. M. Vinokur, *Rev. Mod. Phys*. **66**, 1125 (1994).

[17] E. F. Talantsev, K. Iida, T. Ohmura, T. Matsumoto, W. P. Crump, N. M. Strickland, S. C. Wimbush and H. Ikuta, *Sci. Rep*. **9**, 14245 (2019).

[18] L. Fang, Y. Jia, V. Mishra, C. Chaparro, V. K. Vlasko-Vlasov, A. E. Koshelev, U. Welp, G. W. Crabtree, S. Zhu, N. D. Zhigadlo, S. Katrych, J. Karpinski and W. K. Kwok, *Nat. Commun*. **4**, 2655 (2013).

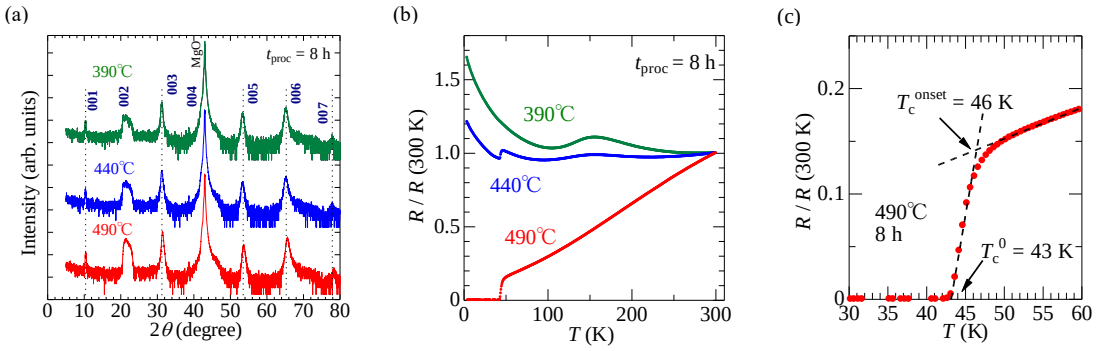

Fig. 1

(a) The $\theta/2\theta$ scans and (b) the temperature dependence of NdFeAsO thin films processed at different temperatures. The dashed lines in Fig. (a) indicate the positions of the 00l peaks of the non-doped NdFeAsO thin film. The processing time (t_{proc}) was fixed at 8 h. (c) The enlarged view near the transition temperature of the superconducting NdFeAs(O,H) thin film shown in (b). T_c^{onset} was determined as the intersection between the linear fit to the normal state resistance and the steepest slope of the resistance, resulting in T_c^{onset} = 46 K. T_c^0 was defined as the intersection between zero resistance and the steepest slope of the resistance, corresponding to T_c^0 = 43 K.

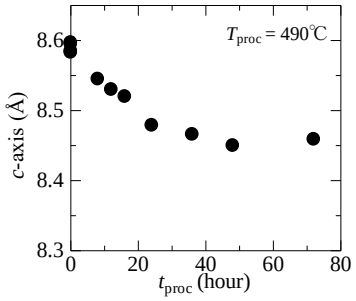

Fig. 2

The c-axis length of NdFeAs(O,H) thin films as a function of the processing time (t_{proc}). The processing temperature was fixed at 490℃.

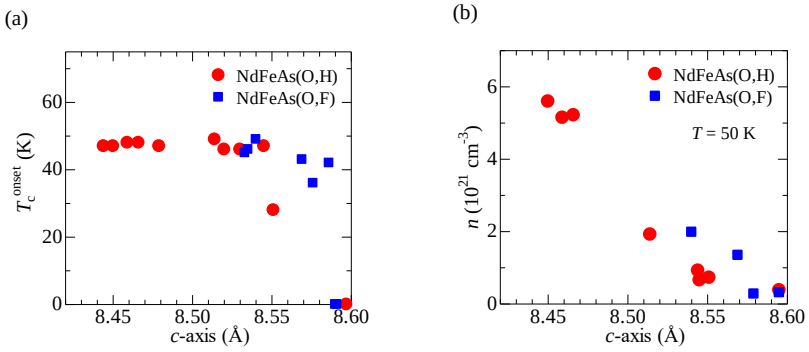

Fig. 3

The c-axis length dependence of (a) T_c^{onset} and (b) the carrier density at 50 K of the NdFeAs(O,H) and NdFeAs(O,F) thin films.

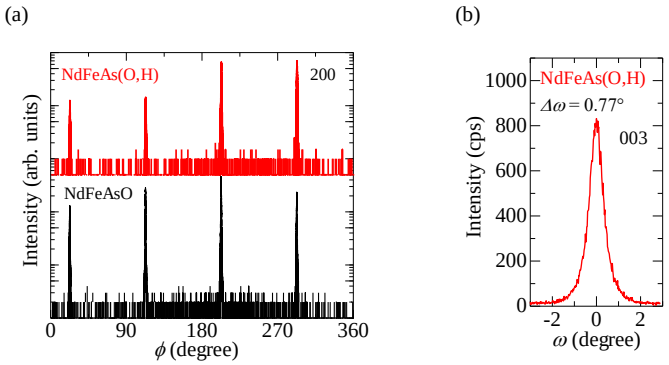

Fig. 4

(a) The 200 peak ϕ scans of the NdFeAsO and NdFeAs(O,H) thin films. (b) The 003 peak rocking curve of the NdFeAs(O,H) film. The NdFeAs(O,H) film was fabricated by the following conditions: T_{proc} = 490°C and t_{proc} = 36 h.

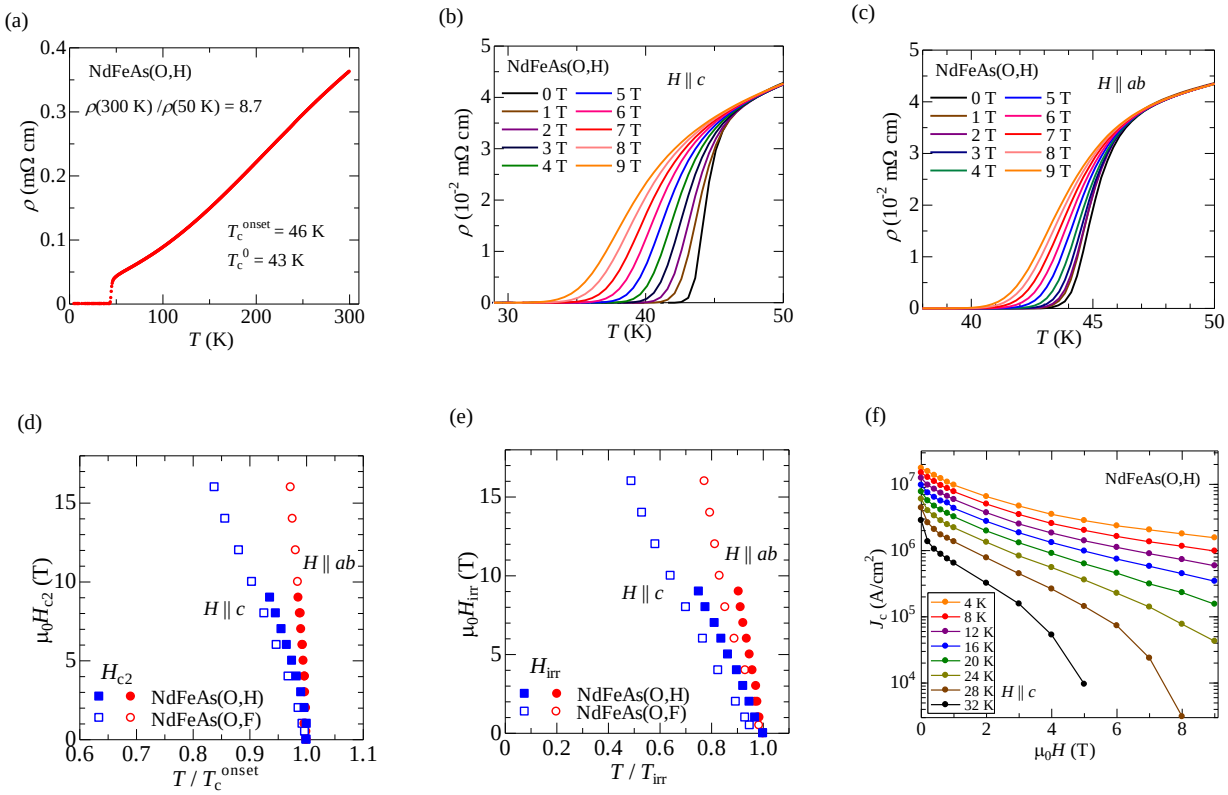

Fig. 5

(a) The temperature dependence of the resistivity of the NdFeAs(O,H) thin film shown in Fig. 4. The ratio of ρ(300 K) to ρ(50 K) was 8.7. The resistivity curves in magnetic fields up to 9 T (b) for $H \parallel c$ and (c) for $H \parallel ab$. (d) The upper critical fields and (e) the irreversibility fields of the NdFeAs(O,H) thin film, evaluated from the data shown in Figs. 5(b) and (c). For comparison, the data of NdFeAs(O,F) [13] are also plotted. (f) J_c-H properties of the film shown in Figs. 5(a)-(c) measured at various temperatures for $H \parallel c$.